FULL PAPER

Benzobisthiazole as Weak Donor for Improved Photovoltaic Performance: Microwave Conductivity Technique Assisted Molecular Engineering

Masashi Tsuji, Akinori Saeki, Yoshiko Koizumi, Naoto Matsuyama, Chakkooth Vijayakumar, and Shu Seki**

New donor–acceptor-type copolymers comprised of benzobisthiazole (BBTz) as a weak donor rather than acceptor are proposed. This approach can simultaneously lead to deepening the HOMO and LUMO of the polymers with moderate energy offset against fullerene derivatives in bulk heterojunction organic photovoltaics. As a proof-of-concept, BBTz-based random copolymers conjugated with typical electron acceptors: thienopyrroledione (TPD) and benzothiadiazole (BT) based on density functional theory calculations are synthesized. Laser-flash and Xe-flash time-resolved microwave conductivity (TRMC) evaluations of polymer:[6,6]-phenyl C_{61} butyric acid methyl ester (PCBM) blends are conducted to screen the feasibility of the copolymers, leading to optimization of processing conditions for photovoltaic device application. According to the TMRC results, alternating BBTz-BT copolymers are designed, exhibiting extended photoabsorption up to ca. 750 nm, deep HOMO (–5.5 to –5.7 eV), good miscibility with PCBM, and inherent crystalline nature. Moreover, the maximized PCE of 3.8%, the top-class among BBTz-based polymers reported so far, is realized in an inverted cell using TiO_x and MoO_x as the buffer layers. This study opens up opportunities to create low-bandgap polymers with deep HOMO, and shows how the device-less TRMC evaluation is of help for decision-making on judicious molecular design.

1. Introduction

Organic photovoltaics (OPV) provide substantial promise for low-cost, lightweight, and bendable solar cells.[1] Recently, notable improvement in the power conversion efficiency (PCE) of 8–12% has been achieved[2] in bulk heterojunction (BHJ) OPVs. This was realized through the development of new semiconducting materials, which concurrently satisfy the prerequisites in optical properties (the overlap of absorbance with the solar spectrum), nanoscale morphology (formation of a p/n network that ensures both charge separation and collection), and energy alignment (low-lying highest occupied molecular orbital (HOMO) level to gain high open-circuit voltage (V_{oc})). The former two properties are associated with the short circuit current (J_{sc}) and partly controlled by processing conditions (solvent, additive, and thermal annealing). In one of the most common design strategies for low-bandgap polymers, the intramolecular charge-transfer phenomenon is rationally utilized through the alternating arrangement of donor (e.g., benzodithiophene (BDT),[3] cychlopentadithiophene (CPDT),[4] carbazole (Cz),[5] fluorene (FLO)[6]) and acceptor (e.g., benzothiadiazole (BT),[7] thienopyrroledione (TPD),[8] isoindigo (IIDG),[9] diketopyrrolopyrole (DKPP)[10]). This design allows lowering of the lowest unoccupied molecular orbital (LUMO) while keeping a deep HOMO of the copolymers.

While new donor and acceptor units are still evolving, combinations of typical units are rapidly being explored. Thiazole derivatives such as BT,[7] bithiazole (bTz),[11] thiazolothiazole (TzTz),[12] and benzobisthiazole (BBTz)[13–16] are regarded as acceptors and have been polymerized with typical donor units. In particular, incorporation of BT or TzTz has succeeded in demonstrating respectably high PCEs of 6–7%. Nevertheless, BBTz has not been subjected to intensive investigation. Jenekhe et al. reported OPVs of BBTz copolymers coupled with typical donors (BDT, CPDT, Cz, bithiophene, dithienopyrole, and Si-CPDT),[14] where the absorption maxima in the film state are less than 560 nm. They tuned the ionization potential to secure oxidation-resistance, leading to a maximized PCE of 3.83% for a BBTz and BDT copolymer:[6,6]-phenyl C_{71} butyric acid methyl ester ($PC_{71}BM$) = 1:2 device.[15] The optical properties of these polymers indicate that BBTz is a weak acceptor, which is also

M. Tsuji, Dr. A. Saeki, Dr. Y. Koizumi,
Dr. N. Matsuyama, Dr. C. Vijayakumar, Prof. S. Seki
Department of Applied Chemistry
Graduate School of Engineering
Osaka University
2-1 Yamadaoka, Suita, Osaka 565-0871, Japan
E-mail: saeki@chem.eng.osaka-u.ac.jp; seki@chem.eng.osaka-u.ac.jp
Dr. A. Saeki
PRESTO, Japan Science and Technology Agency (JST)
4-1-8 Honcho Kawaguchi, Saitama 332-0012, Japan
Dr. Y. Koizumi
RIKEN Advanced Science Institute
2-1 Hirosawa, Wako, Saitama 351-0198, Japan

DOI: 10.1002/adfm.201301371

dictated from its HOMO and LUMO levels calculated by density functional theory (DFT).

Here, we focused on the use of BBTz as a weak donor rather than acceptor and designed new copolymers in conjunction with typical acceptors (BT and TPD). This design is expected to yield both low bandgap and deep HOMO, which is schematically illustrated in **Figure 1** a (the HOMO and LUMO levels of monomer π-units are given in the Supporting Information, Figure S1a). Commonly a combination of two acceptors, however, leads to an n-type property,[17] because the LUMO of the copolymer is excessively lowered, being unable to preserve energy offset from LUMO of fullerene (empirically > 0.3 eV) to ensure efficient electron transfer.[18] For instance, Wudl et al. systematically investigated the impact of acceptor strength on the electronic and optical properties of donor–acceptor polymers consisting of DKPP coupled with benzene, BT, or benzobisthiadiazole (BBTdz).[19] They revealed ambipolar FET operation for DKPP-BBTdz copolymer which has HOMO at –4.55 eV and LUMO at –3.9 eV (from cyclic voltammetry and photoabsorption onset), pointing out DKPP as a weak donor and BBTdz as an acceptor. Quite recently, Jenekhe et al. reported the use of TzTz and BBTz as a weak donor, which was coupled with electron-withdrawing DKPP unit,[16] and demonstrated a high field-effect transistor (FET) hole mobility of 1.3 $cm^2\ V^{-1}\ s^{-1}$ with 3.4% PCE for TzTz–DKPP polymer and $PC_{71}BM$ blends. However, BBTz–DKPP:$PC_{71}BM$ showed a PCE of just 2.7% with three-order lower FET mobility and an amorphous nature, indicating that the use of BBTz as donor is not readily advantageous. On the contrary, we succeeded in realizing a BBTz (donor)–BT (acceptor) polymer suitable for OPV application, possessing appropriate energy alignment, crystallinity, and inherent high photo-response, resulting in 3.84% PCE for a $PC_{61}BM$ blend (not $PC_{71}BM$). Throughout the study, flash-photolysis time-resolved microwave conductivity (TRMC)[20–22] was utilized to characterize the optoelectronic performance of the copolymers. More importantly, it was also used as a tool for decision-making on the molecular design strategy.

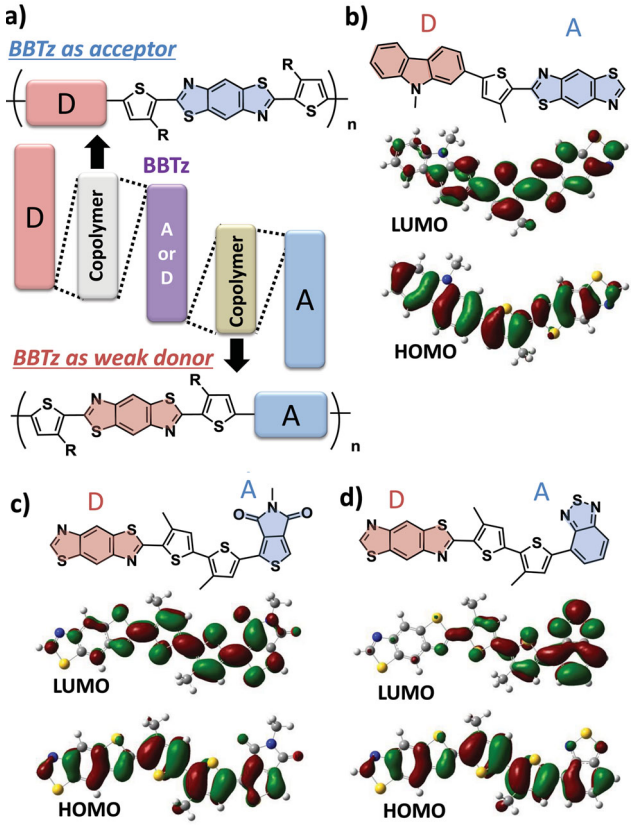

Figure 1. a) Conceptual illustration of building block combinations with respective energy levels, where BBTz is used as an acceptor (upper) and as a weak donor (lower). HOMO and LUMO of: b) Cz (donor)-BBTz (acceptor), c) BBTz (donor)–TPD (acceptor), and, d) BBTz (donor)-BT (acceptor) dimers calculated by DFT using B3LYP/6-31G(d,p).

2. Results and Discussion

2.1. Random Copolymers for Backbone Screening

BBTz was synthesized by the acid-catalyzed condensation of 3-alkylthiophene aldehyde and 2,5-diamino-1,4-benzenedithiol, affording bis(2-thienyl)benzobisthiazole. As a result, the BBTz unit is sandwiched by two thiophenes of which the alkyl side-chains help dissolving the monomer as well as the polymers in organic solvents.[13] As a proof-of-concept, we performed DFT calculation of donor–acceptor dimers of bis(thiophene)-BBTz in conjugation with Cz, TPD, and BT. Figure 1b shows the HOMO and LUMO of BBTz–Cz dimer, which is a combination of normal donor (Cz) and acceptor (BBTz) moieties. The LUMO is biased on the BBTz unit, while the HOMO is spread over the entire molecule. In contrast, the LUMOs of BBTz-TPD (Figure 1c) and BBTz-BT (Figure 1d) dimers are localized on TPD and BT, respectively, in spite of the similarly extended HOMO. The localization of LUMO on TPD or BT is more obvious in DFT results of longer polymer chain (vide infra). The calculated LUMO level of bis(2-thienyl)-BBTz (T-BBTz-T) is higher than those of bis(2-thienyl)-BT (T-BT-T) and bis(2-thienyl)-TPD (T-TPD-T) (Supporting Information, Figure S1b). These observations support our assumption that BBTz can work as a weak donor, relevant to the indication by Wudl et al. that the categorization of "donor" and "acceptor" moieties is not entirely definitive.[19]

Accordingly, two random copolymers of PBBTz-*ran*-TPD and PBBTz-*ran*-BT were synthesized together with a reference polymer (PBBTzCz). The chemical structures of the polymers are shown in **Figure 2**a. The detailed synthetic routes are provided in the Supporting Information. PBBTz-*ran*-TPD and PBBTz-*ran*-BT were prepared by Stille coupling with stannylthiophene (T) at BBTz:T:TPD (BBTz:T:BT) = 1:2:1 molecular ratio. The electronic absorption spectra of PBBTz-*ran*-TPD and PBBTz-*ran*-BT exhibited maxima at identical positions (517 nm, Figure 2b), which is 60 nm longer than that of PBBTzCz. The maxima in film states were marginally red-shifted, indicative of planarization of polymer backbone. The HOMO and LUMO levels of these polymers were measured by photoelectron yield spectroscopy (PYS), and photoabsorption edges (Supporting Information, Figure S2). Importantly, the HOMO levels of the random copolymers and PBBTzCz are deep (–5.7 eV) as listed in **Table 1**, highlighting the weak-donor role in these polymers.

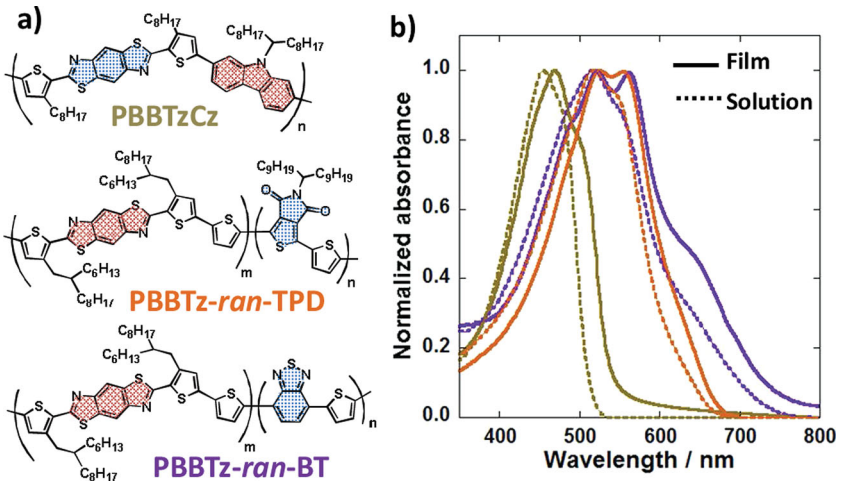

Figure 2. a) Chemical structures of the reference (PBBTzCz) and random polymers (PBBTz-*ran*-TPD and PBBTz-*ran*-BT). The pink and white blue represent donor and acceptor moieties, respectively. b) Normalized photoabsorption spectra of PBBTzCz (ocher), PBBTz-*ran*-TPD (orange), and PBBTz-*ran*-BT (purple). The solid lines are chloroform solutions and the dotted lines are films on quartz.

The photo-conductive properties of PBBTzCz, PBBTz-*ran*-TPD, and PBBTz-*ran*-BT films were surveyed by means of laser-flash TRMC[20] with an excitation wavelength of 355 nm. **Figure 3**a displays the dependences of the transient photoconductivity maxima ($\varphi\Sigma\mu_{max}$) and its half-lifetime ($\tau_{1/2}$) on the blend ratio of PBBTzCz and [6,6]-phenyl C_{61} butyric acid methyl ester ($PC_{61}BM$). The corresponding kinetic traces are provided in Figure S3, Supporting Information. $\varphi\Sigma\mu$ is the product of ϕ and $\Sigma\mu$, where φ is the charge carrier generation efficiency and $\Sigma\mu$ is the sum of positive (μ+) and negative (μ-) charge-carrier mobilities. Higher $\varphi\Sigma\mu_{max}$ and longer $\tau_{1/2}$ can lead to better OPV performance, as proved in regioregular poly(3-hexylthiophene) (P3HT):$PC_{61}BM$ blends, because the product of $\varphi\Sigma\mu_{max}$ and $\tau_{1/2}$ values reflects the effective total number of charges collected by the electrodes.[21] PBBTzCz:$PC_{61}BM$ blend films exhibited the maximum $\varphi\Sigma\mu_{max}$ at around 1:1-1:3, while $\tau_{1/2}$ always stays at a very small level. It should be noted that $\varphi\Sigma\mu_{max}$ was increased by six times upon addition of $PC_{61}BM$ concomitant with a progressive fluorescence quenching (Supporting Information, Figure S4), demonstrating an efficient exciton migration to p/n interfaces and subsequent charge separation. On the other hand, the $\varphi\Sigma\mu_{max}$ of PBBTz-*ran*-TPD:$PC_{61}BM$ blend was increased by only a factor of two, along with still small $\tau_{1/2}$ (Figure 3b). This is explained by a bound intermolecular (interfacial) charge-transfer state[23,24] and/or prompt geminate charge recombination,[25] which does not contribute to free charge-generation. Notably, PBBTz-*ran*-BT:$PC_{61}BM$ blend films revealed marked enhancement in both $\phi\Sigma\mu_{max}$ and $\tau_{1/2}$, the maxima of which simultaneously located at p/n = 1:2, as shown in Figure 3c.

Following the prescreening results by TRMC, we fabricated OPV devices of PBBTzCz, PBBTz-*ran*-TPD, and PBBTz-*ran*-BT with respectively optimized mixing ratios with $PC_{61}BM$. After optimization of processing conditions (solvent, thermal annealing, and solvent additive: 1,8-diiodooctane, DIO), PBBTzCz and PBBTz-*ran*-TPD resulted in PCEs of 0.95 and 0.90% with relatively high V_{oc} of 0.74 and 0.72 V, respectively (Figure 3d). Other device parameters are summarized in Table 1. The PCE of PBBTzCz was one order higher than that of the identical backbone with different alkyl chains reported by Jenekhe et al. (0.06%).[14] This could be simply attributed to the more precise formation of BHJ network.

Atomic force microscope (AFM) images of the devices show the formation of BHJ structures at nanometer dimensions (Supporting Information, Figure S5a–d). Although the PCE values are almost competitive, PBBTzCz gave higher J_{sc} and lower fill factor (FF) than those of PBBTz-*ran*-TPD. The current density of PBBTzCz is still increasing under reverse bias, suggesting that charge-carriers are initially generated at higher density, but they recombine even at short-circuit conditions, leading to a low FF (0.30). Conversely, PBBTz-*ran*-TPD displayed a higher FF (0.56), but the J_{sc} is low, due to inefficient initial charge separation. These device characterizations are in a good agreement with TRMC results. However, PBBTz-*ran*-BT failed to indicate an OPV character, mainly ascribed to the strong aggregating nature, as evident from an extremely rough morphology observed even by an optical microscope (Supporting Information, Figure S5d).

2.2. Alternating Copolymers Aimed for Raising OPV Performance

Despite the failure in device fabrication, we chose the BT unit rather than TPD for further investigation, because

Table 1. Molecular weight, optoelectronic properties, and OPV device parameters of PBBTzCz, PBBTz-*ran*-TPD, and PBBTz-*ran*-BT.

Polymer	$\overline{M}_w$ [kg mol^{-1}]	PDI[a]	λ_{max}[b] (film) [nm]	HOMO[c] [eV]	LUMO[c] [eV]	PCE [%]	V_{oc} [V]	J_{sc} [mA cm^{-2}]	FF
PBBTzCz	5	1.8	457 (469)	– 5.7	– 3.2	0.95[d]	0.74[d]	4.21[d]	0.30[d]
PBBTz-*ran*-TPD	23	2.5	517 (524)	– 5.7	– 3.9	0.90[e]	0.72[e]	2.25[e]	0.56[e]
PBBTz-*ran*-BT	32	6.3[f]	517 (522)	– 5.7	– 3.9	– [g]	– [g]	– [g]	– [g]

[a]Polydispersity index; [b]Chloroform solution; [c]HOMOs were measured by PYS; LUMOs were calculated from the band edge of the film absorption; [d]Polymer:$PC_{61}BM$ = 1:2 (w/w); an *o*-dichlorobenzene (oDCB) solution, thermal annealing at 100 °C for 10 min; [e]Polymer:$PC_{61}BM$ = 1:1 (w/w); oDCB solution with 3% v/v DIO, thermal annealing at 150 °C for 10 min; [f]Bimodal; [g]Not obtained.

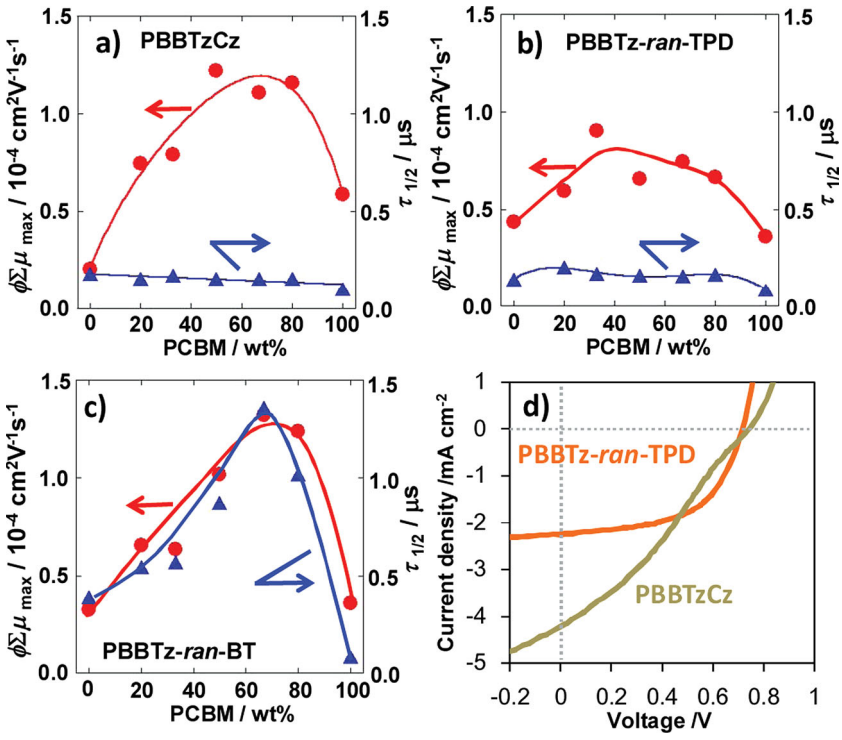

Figure 3. Photoconductivity transient maximum ($\varphi\Sigma\mu_{max}$, red circles, left axis) and its half-lifetime ($\tau_{1/2}$, blue triangles, right axis) measured by laser-flash TRMC upon exposure to 355 nm in a) PBBTzCz:$PC_{61}BM$ blends, b) PBBTz-*ran*-TPD:$PC_{61}BM$ blends, and, c) PBBTz-*ran*-TPD:$PC_{61}BM$ blends. d) *J–V* curves of PBBTzCz:$PC_{61}BM$ = 1:2 (ocher) and PBBTz-*ran*-TPD:$PC_{61}BM$ = 1:1 (orange) devices (ITO/PEDOT:PSS/active layer/Ca/Al) under one sun illumination.

PBBTz-*ran*-BT revealed a much better TRMC profile than PBBTz-*ran*-TPD. 3-alkylthiophenes having branched long alkyl chains were coupled at the 5-position with BT, allowing for good solubility as well as high planarity arising from the avoidance of steric hindrance at the BT and thiophene junction.[26] Accordingly, the stannyl-BBTz was polymerized with the bis(alkylthiophene)-BT units, affording PBBTzBT-HD (2-hexyl-decyl:C_6-C_{10}) and PBBTzBT-DT (2-decyl-tetradecyl: C_{10}-C_{14}) with high molecular weights (**Figure 4**a). The absorption maxima in solution were further red-shifted to 569 and 598 nm for PBBTzBT-HD and PBBTzBT-DT, respectively, and an extra 20–40 nm shift was observed in the film states accompanied by distinct vibronic peaks (Figure 4b). The HOMO energies are considerably deep (–5.5 and –5.7 eV) with appropriate LUMO levels (–3.8 and –3.9 eV). The optical and electrochemical properties are summarized in **Table 2**.

More pronounced improvement in films is recognized in the X-ray diffraction (XRD) spectra shown in Figure 4c. PBBTzBT-HD exhibited an intense and sharp peak at $2\theta = 4.04°$ (*d*-spacing = 21.9 Å) along with its second-order peak at 8.18°, relevant to the intermolecular distance between polymer chains interdigitated by side alkyl chains. The *d*-spacing of PBBTzBT-DT was widened by 13% to 24.7 Å ($2\theta = 3.58°$) consistent with the extended chain length, but the peaks are still strong, given the second-order diffraction peaks. This indicates an intriguing intermolecular π-stacking of PBBTzBT-HD and PBBTzBT-DT, in contrast to the much broader and weaker diffraction patterns of PBBTzCz (*d* = 18.5 Å), PBBTz-*ran*-TPD (*d* = 21.8 Å), and PBBTz-*ran*-BT (*d* = 19.8 Å).

Of particular importance for PBBTzBT-HD and PBBTzBT-DT is the linear conformation of polymer backbone. Bis(thiophene)-BT and bis(thiophene)-BBTz are an axisymmetric and centrosymmetric units,[27] respectively; however, their alternating copolymers cancel the bond angle and they are regarded as a linear shape, which most likely leads to strong π-stacking and enhancement of intermolecular[27] and intramolecular[28] charge transports. Coulomb-attenuating method (CAM)-DFT[29] of the modeled oligomer of PBBTzBT shown in Figure 4d clearly demonstrates its extended feature, where the HOMO is delocalized over 5 nm (more than two repeating units) and instead, the LUMO is converged on the central BT unit, reiterating that BT acts as an acceptor. The similar DFT calculations were performed for the model of PBBTz-*ran*-TPD and PBBTzCz polymers (Supporting Information, Figure S6). Their LUMOs are localized on the respective acceptor units (TPD or BBTz), and more importantly, their conformations take an arch or winding shape. Time-dependent CAM-DFT of PBBTzBT provides the assignment of electronic transition in the absorption spectra (Supporting Information, Figure S6). The peaks at the longest wavelength (ca. 600 nm) shown in Figure 4b is mainly due to the transition from HOMO to LUMO involved by intramolecular charge transfer (ICT) nature;[30] the second peak at around 480 nm is partly ascribed to HOMO–2 to LUMO+2 and HOMO-1 to LUMO+1, mainly originated from the bis(thiophene)-BT unit.

Prior to device fabrication, the values of $\varphi\Sigma\mu_{max}$ and $\tau_{1/2}$ were examined by TRMC (The kinetic traces of photoconductivity transients are provided in Figure S8, Supporting Information). As shown in **Figure 5**a, $\varphi\Sigma\mu_{max}$ of PBBTzBT-HD increased by three times compared with those of PBBTzCz, PBBTz-*ran*-TPD, and PBBTz-*ran*-BT. Interestingly, PBBTzBT-HD exhibited two peaks at $PC_{61}BM$ = 20 and 67 wt%, which has been also observed for typical conjugated polymers such as P3HT, poly[*N*-9''-hepta-decanyl-2,7-carbazole-*alt*-5,5-(4',7'-di-2-thienyl-2',1',3'-benzothiadiazole)] (PCDTBT), and poly[2,6-(4,4-bis-(2-ethylhexyl)-4*H*-cyclopenta[2,1-*b*;3,4-*b*']dithiophene)-*alt*-4,7(2,1,3-benzothiadiazole)] (PCPDTBT).[22] This is due to an interplay of hole mobility, electron mobility, and their photogeneration yield at different p/n blend ratio. However, $\tau_{1/2}$ gave the sole maximum at $PC_{61}BM$ = 67 wt% and, thus, the OPV device was fabricated at this blend ratio (PBBTzBT-HD:$PC_{61}BM$ = 1:2). With an identical optimization of processing to the previous cases, 3.20% PCE was achieved with high V_{oc} of 0.83 V (Table 2), much superior to the random polymer (PBBTz-*ran*-BT) and the reference (PBBTzCz), in accordance with TRMC prediction. This improvement is rationalized by the linear backbone conformation implemented by alternating polymerization as well as the increased molecular weight with low PDI, extended

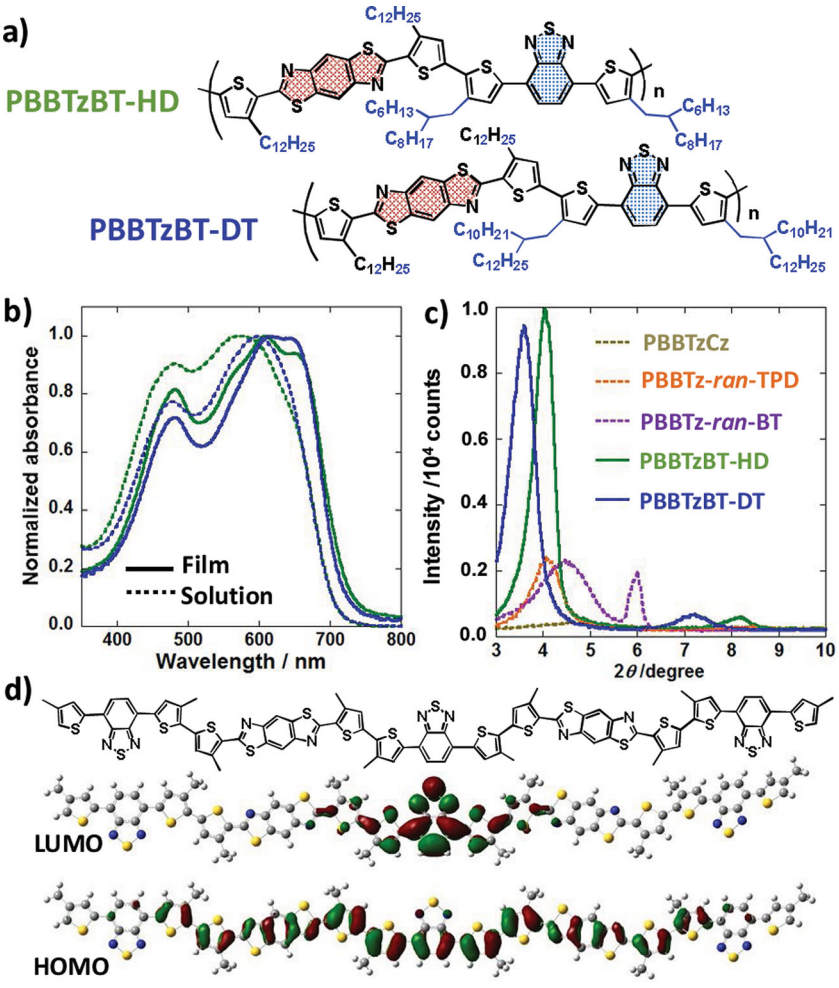

Figure 4. a) Chemical structures of alternating copolymers. The pink and white blue represent donor and acceptor moieties, respectively. HD and DT stand for the side-alkyl chains drawn in blue. b) Normalized photoabsorption spectra of PBBTzBT-HD (green) and PBBTz-DT (blue). The solid lines are chloroform solutions and the dotted lines are films on quartz. c) XRD patterns of the pristine copolymers. d) HOMO and LUMO of PBBTzBT-modeled oligomer after geometry optimization by CAM-DFT using B3LYP/6-31G(d,p).

photoabsorption, and good BHJ network formation (AFM images in Figure S9, Supporting Information).

Addressing the solubility issues of PBBTzBT-HD as reflected in the polymerization yield, four-extended alkyl chains were introduced into the polymer as PBBTzBT-DT, and its photoconductive properties were investigated by TRMC. It is striking to note that both $\phi\Sigma\mu_{max}$ and $\tau_{1/2}$ were further enhanced by a factor of three (Figure 5b). They displayed distinct one maximum, but at different blend ratio (1:1 for $\phi\Sigma\mu_{max}$ and 1:4 for $\tau_{1/2}$). Therefore we performed TRMC using white light pulses from a solar-simulating Xe-flash lamp as a photoexcitation source, the so-called Xe-flash TRMC.[22] It has been recently developed for evaluation of material feasibility in OPV devices, where the photoconductivity maximum ($\Delta\sigma_{max}$) includes not only the generation yield and local mobility of charge carrier but also its lifetime and light-harvesting property of the film under much lower photo-irradiation density than that of laser-flash TRMC. As a result, PBBTzBT-DH: $PC_{61}BM$ deciphered the best blend ratio of 1:2 (Figure 5c).

Further optimization of solvents, additives, thermal annealing conditions, and thickness of an active layer were screened rapidly based on TRMC measurements, giving a maximized PCE of 2.37%. However, this is lower than PBBTzBT-HD in spite of good p/n mixing (AFM in Figure S9 and fluorescence quenching in Figure S10, Supporting Information), mainly due to the decreased J_{sc} (Table 2). On a closer look at the *J–V* curve in Figure 5d, PBBTzBT-DT exhibits an S-kink shape at the open-circuit voltage. This could be linked to the following: i) nongeminate charge recombination loss via charge trap by impurities,[31] ii) imbalance between hole and electron mobilities intimately related to BHJ structure,[32] and, iii) contact resistance at the BHJ/buffer layer interface.[33] The third one is thought plausible, since the HOMO of PBBTzBT-DT was substantially deepened to –5.7 eV and, moreover, TRMC results suggest a better performance of PBBTzBT-DT than PBBTzBT-HD. Thus we modified the device structure by replacing the anode buffer layer consisting of typical PEDOT:PSS.

Table 2. Molecular weight, opto-electronic properties, and OPV device parameters of PBBTzBT-DH and PBBTzBT-DT.

Polymer	$\overline{M}_w$ [kg mol^{-1}]	PDI[a)]	λ_{max}[b)] (film) [nm]	HOMO[c)] [eV]	LUMO[c)] [eV]	PCE [%]	V_{oc} [V]	J_{sc} [mA cm^{-2}]	FF
PBBTzBT-HD	35	1.2	569 (609)	–5.5	–3.8	3.20[d)]	0.83[d)]	7.17[d)]	0.54[d)]
PBBTzBT-DT	107	2.1	598 (619)	–5.7	–3.9	2.37[e)]	0.83[e)]	5.74[e)]	0.50[e)]
						3.84[f)]	0.84[f)]	8.01[f)]	0.57[f)]

[a)]Polydispersity index; [b)]Chloroform solution; [c)]HOMO were measured by PYS; LUMOs were calculated from the absorption band edge of film; [d)]Polymer:$PC_{61}BM$ = 1:2 (w/w); oDCB solution; [e)]Polymer:$PC_{61}BM$ = 1:2 (w/w); a chlorobenzene (CB) solution with 3% v/v DIO, thermal annealing at 160 °C for 10 min; [f)]Inverted cell (ITO/TiO_x/BHJ/MoO_x/Au); polymer:$PC_{61}BM$ = 1:2 (w/w); CB solution with 3% v/v DIO, thermal annealing at 120 °C for 10 min.

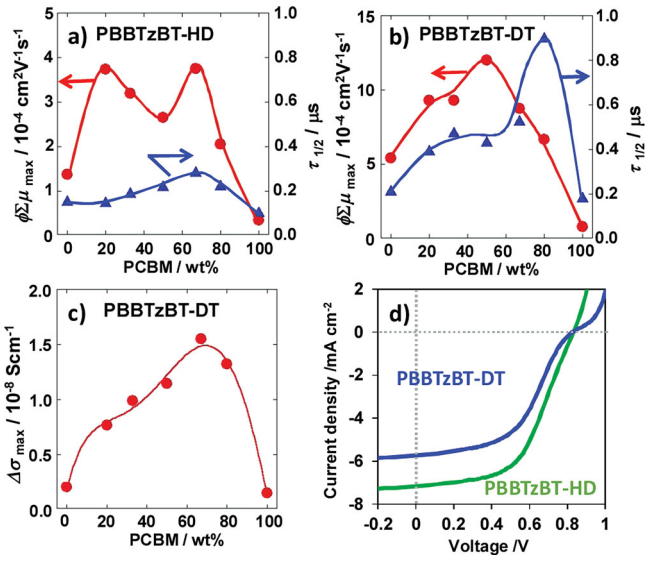

Figure 5. Photoconductivity transient maximum ($\phi\Sigma\mu_{max}$, red circles, left axis) and its half-lifetime ($\tau_{1/2}$, blue triangles, right axis) measured by laser-flash TRMC upon exposure to 355 nm found in: a) PBBTzBT-HD:$PC_{61}BM$ blends, and, b) PBBTzBT-DT:$PC_{61}BM$ blends. c) $\Delta\sigma_{max}$ of PBBTzBT-DT:$PC_{61}BM$ blend films measured by Xe-flash TRMC using white light pulse as an excitation. d) *J–V* curves of PBBTzBT-HD:$PC_{61}BM$ = 1:2 (green) and PBBTzBT-DT:$PC_{61}BM$ = 1:2 (blue) devices (ITO/PEDOT:PSS/active layer/Ca/Al) under one sun condition.

2.3. Inverted Cell of PBBTzBT-DT

Encouraged by the TRMC studies on PBBTzBT-DT, we fabricated an inverted cell composed of MoO_x/Au anode and TiO_x/ITO cathode. The energy diagrams of normal and inverted cells are depicted in **Figure 6**a.[34] In the normal cell, the HOMO of PBBTzBT-DT (–5.7 eV) is much deeper than the work function of PEDOT:PSS (–5.1 eV). This might form interfacial barriers,[33] leading to the lower J_{sc} and FF. On the other hand, the work function of MoO_x is –5.4 eV,[34] which reduces the gap with the HOMO. A TiO_x layer prepared by the sol–gel technique was used as a cathode buffer layer on an ITO electrode.[35] This inverted cell structure is underlined by the successful examples reported in polymers:fullerene[34] and small molecule:fullerene[36] BHJ, in particular, the cell system with p-type semiconductors with deep-lying HOMO. As shown in Figure 6b, a good p/n mixing was successfully formed on the TiO_x layer under the same processing condition with the normal cell (chlorobenzene with 3% v/v DIO). As a consequence, the best PCE of 3.84% was realized with enhanced J_{sc} (8.01 mA cm^{-2}) and FF (0.57) as given in Table 2. Notably, the *J–V* curve in Figure 6c demonstrates the extinction of an S-kink with the lowest series resistance (5.0 Ω cm^2), supportive of the improved interfacial contact.

Figure 6d shows the device performance of PCE divided by V_{oc} (= J_{sc} × FF) as a function of $\varphi\Sigma\mu_{max}$ of laser-flash TRMC. Interestingly, we found an excellent correlation between them as has been observed in the representatives of low-bandgap polymers,[22] highlighting TRMC measurements as a versatile technique not only for optimization of processing condition but also for feedback on the material design. An emphasis is given to that the PCE/V_{oc} of normal cell of the last polymer, PBBTzBT-DT, was much lower than the upward trend observed in other polymers. However its inverted cell increased the value of PCE/V_{oc}, giving a sublinear dependence on $\varphi\Sigma\mu_{max}$ which can interpolate all of the investigated polymers. Therefore this study brought out the usefulness of device-less TRMC evaluation to guide designing the material and predicting its device performance.

3. Conclusion

We designed new low-bandgap polymers composed of BBTz as a weak donor rather than acceptor conjugated with strong acceptors, TPD and BT. Firstly, the random copolymers, PBBTz-*ran*-TPD and PBBTz-*ran*-BT, were synthesized in order to judge the superior backbone. The photoconductivities of their blends with $PC_{61}BM$ were examined by laser-flash TRMC, indicating a better optoelectronic property in combination with BT. On the contrary, PBBTz-*ran*-BT:$PC_{61}BM$ gave no device output, due to its poor film processiblity, while PBBTz-*ran*-TPD exhibited a PCE of 0.90%, almost similar to the reference polymer of PBBTzCz (BBTz is a weak acceptor in this case). However, on the basis of TRMC prediction, we subsequently synthesized alternating copolymers of BBTz-BT, affording crystalline PBBTzBT-HD and PBBTzBT-DT with red-shifted photoabsorption. The former exhibited a PCE of 3.20% with a high V_{oc} of 0.83 V; however, the latter resulted in 2.37%, in spite of its largest TRMC signal. Considering the TRMC experiments, the deep HOMO (–5.7 eV), and observed an S-kink in the *J–V* curve, we finally fabricated an inverted cell of PBBTzBT-DT and succeeded in boosting the PCE to 3.84%, which is top-class among the BBTz-based polymers so far. The approach using BBTz as a weak donor opens a versatile route toward low-bandgap polymers with deep HOMO, and more importantly, we showed that TRMC is a useful guide for molecular design as well as for optimization of processing conditions.

4. Experimental Section

General: Steady-state photoabsorption spectroscopy was performed using a Jasco V-570 UV-vis spectrophotometer. Chemicals and solvents were purchased from Tokyo Chemical Inc. (TCI) and Kishida Chemical Inc., respectively, unless otherwise noted. PYS experiments were carried out by a RIKEN Keiki Co. Ltd. model AC-3. XRD measurements were done on a Rigaku RINT ultra X18SAXS-IP (Cu Kα: 1.5418 Å). AFM analyzes were performed by a Seiko Instruments Inc. model Nanocute OP and Nanonavi II. DFT calculations were performed by a Gaussian 09 Rev.A02 package.

Synthesis of Polymers: The synthesis of monomers and characterization by NMR spectroscopy is provided in the Supporting Information. Details of the polymerization are also given in the Supporting Information. The tin compounds were purified prior to coupling reaction by a recycling preparative HPLC system on a Japan Analytical Industry Co., Ltd. LC-9210NEXT with JaiGel-1H/-2H (eluent $CHCl_3$). PBBTzCz was synthesized by Suzuki coupling of brominated bisthiophene-BBTz and bis(boronic acid pinacol ester)carbazole in vigorously degassed toluene/aqueous K_2CO_3 at 135 °C in the presence of Aliquat 336. The yield after purification was as low as 6%. PBBTz-*ran*-TPD and PBBTz-*ran*-BT were polymerized by Stille coupling of bis(tributylstanyl)-thiophene

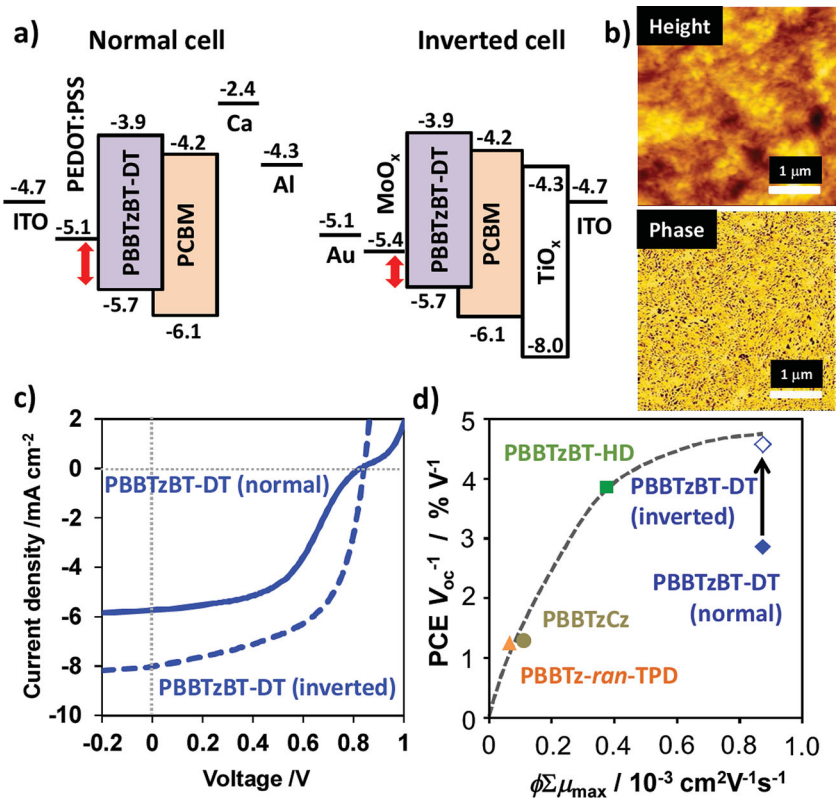

Figure 6. a) Energy diagrams of (left) normal and (right) inverted structures. b) AFM (upper) height and (lower) phase images of the optimized PBBTzBT-DT:$PC_{61}BM$ = 1:2 film. The scale bar corresponds to 1 μm. c) *J–V* curves of PBBTzBT-DT:$PC_{61}BM$ = 1:2 devices under one sun condition. The solid and dotted lines represent the normal and inverted structures, respectively. d) Correlation between PCE V_{oc}^{-1} (=J_{sc} × FF) of the optimized OPV devices and corresponding $\phi\Sigma\mu_{max}$ of the blend films measured by laser-flash TRMC excited at 355 nm. The arrow indicates the improvement of PBBTzBT-DT:$PC_{61}BM$ device by changing normal cell to inverted cell. The dotted line is a visual guide.

(50 mol%), brominated-BBTz (25 mol%), and brominated TPD or BT (25 mol%) in degassed toluene at 130 °C. The yields of PBBTz-*ran*-TPD and PBBTz-*ran*-BT after purification were 93% and 11%, respectively. PBBzBT-HD and PBBzBT-DT were synthesized by Stille coupling of bis(tributylstanylthiophene)-BBTz and brominated bis(alkylthiophene)-BT in chlorobenzene/dimethylformamide at 110 °C. The yields after purification were 13% and 81%, respectively. Molecular weights of polymers were determined using the gel permeation chromatography (GPC) method with polystyrene standards. GPC analysis was performed with polymer/tetrahydrofuran (THF) (HPLC grade) solution at a flow rate of 1 cm^3 min^{-1} at 40 °C, on a HITACHI L-2130, L-2455, L-2530 chromatography instrument with Shodex KF-804L/KF-805L (Shodex Co., Japan) connected to a refractive index detector.

Time-Resolved Microwave Conductivity (TRMC): A resonant cavity was used to obtain a high degree of sensitivity in the conductivity measurement. The resonant frequency and microwave power were set at ca. 9.1 GHz and 3 mW, respectively, so that the electric field of the microwave was sufficiently small to not disturb the motion of charge carriers. Third harmonic generation (THG; 355 nm) of a Nd:YAG laser (Continuum Inc., Surelite II, 5–8 ns pulse duration, 10 Hz)[20,21] or microsecond white light pulse from a Xe flash lamp was used as an excitation source.[22] The photoconductivity $\Delta\sigma$ was obtained by $\Delta P_r/(AP_r)$, where ΔP_r, A, and P_r are the transient power change of reflected microwave from a cavity, the sensitivity factor, and the reflected microwave power, respectively. The nanosecond laser intensity was set at 4.6×10^{15} photons cm^{-2} $pulse^{-1}$. The power of the white light pulse was 0.3 mJ cm^2 $pulse^{-1}$.

The samples were drop-casted on a quartz plate from solutions of polymer and $PC_{61}BM$ and dried in a vacuum oven. After the preparation of thin films, the films were thermally annealed on a hot plate. The TRMC experiments were performed under ambient conditions at room temperature.

Organic Photovoltaic Cells: A PEDOT:PSS (Heraeus Clevios P VP AI 4083) layer was cast onto the cleaned ITO layer by spin-coating after passing through a 0.2 μm filter. The substrate was annealed on a hot plate at 150 °C for 30 min. An active layer consisting of polymer and $PC_{61}BM$ (purchased from Frontier Carbon Inc.) was cast on top of the PEDOT:PSS buffer layer in a nitrogen glove box by spin-coating after passing through a 0.2 μm filter. The thickness was around 100 nm. A cathode consisting of 20 nm Ca and 100 nm Al layers was sequentially deposited through a shadow mask on top of the active layers by thermal evaporation in a vacuum chamber. The resulting device configuration was ITO (120–160 nm)/PEDOT:PSS (45–60 nm)/active layer (ca. 100 nm)/Ca (20 nm)/Al (100 nm) with an active area of 7.1 mm^2. In an inverted cells, diluted TiO_x precursor (Koujundo Kagaku Corp.) was cast on the ITO layer by spin-coating after passing through a 0.2 μm filter. The layers were annealed on a hot plate at 150 °C for 10 min. A polymer:$PC_{61}BM$ active layer was cast in a similar fashion as that for the normal OPV. The anode consisted of 10 nm MoO_x and 50 nm Au layers that was sequentially deposited through a shadow mask on top of the active layers by thermal evaporation of MoO_3 and Au in a vacuum chamber. The resulting device configuration was ITO (120–160 nm)/TiO_x (ca. 10 nm)/active layer (ca. 100 nm)/MoO_x (10 nm)/Au (50 nm) with an active area of 7.1 mm^2. Current–voltage (*J –V*) curves were measured using a source-measure unit (ADCMT Corp., 6241A) under AM 1.5 G solar illumination at 100 mW cm^{-2} (1 sun) using a 300 W solar simulator (SAN-EI Corp., XES-301S).

Supporting Information

Supporting Information is available from the Wiley Online Library or from the author. Details of synthesis of polymers and monomers, calculated HOMO/LUMO energies of monomers (Figure S1), PYS data (Figure S2), photoconductivity transients observed in polymer:$PC_{61}BM$ blend films (Figures S3,S8), fluorescence quenching results (Figures S4,S10), AFM and optical microscopy images (Figures S5,S9), the lobe images of molecular orbitals of PBBTzBT oligomer calculated by TD-CAM-DFT (Figure S6), and calculated HOMO/LUMO of PBBTz-ran-TPD and PBBTzCz oligomers (Figure S7).

Acknowledgements

This work was supported by the Precursory Research for Embryonic Science and Technology (PRESTO) program, the tenure-track program of the Japan Science and Technology Agency (JST), and a KAKENHI grant from the Ministry of Education, Culture, Sports, Science, and Technology (MEXT) of Japan. The authors thank Prof. Atsushi Wakamiya, Hidetaka Nishimura, and Prof. Yasujiro Murata at the Institute for Chemical Research, Kyoto University, Japan, for the use of the AC3 system.

Received: April 23, 2013
Revised: June 5, 2013
Published online: July 17, 2013

[1] Recent reviews: a) B. E. Hardin, H. J. Snaith, M. D. McGehee, *Nat. Photon.* **2012**, *6*, 162; b) G. Li, R. Zhu, Y. Yang, *Nat. Photon.* **2012**, *6*, 153; c) A. Mishra, P. Bäuerle, *Angew. Chem. Int. Ed.* **2012**, *51*, 2020; d) H. J. Son, B. Carsten, I. H. Jung, L. Yu, *Energy Environ. Sci.* **2012**, *5*, 8158; e) D. Credgington, J. R. Durrant, *J. Phys. Chem. Lett.* **2012**, *3*, 1465; f) H. Zhou, L. Yang, W. You, *Macromolecules* **2012**, *45*, 607; g) P. M. Beaujuge, J. M. J. Fréchet, *J. Am. Chem. Soc.* **2011**, *133*, 20009; h) Y. Liang, L. Yu, *Acc. Chem. Res.* **2010**, *43*, 1227.

[2] a) L. Dou, J. Gao, E. Richard, J. You, C.-C. Chen, K. C. Cha, Y. He, G. Li, Y. Yang, *J. Am. Chem. Soc.* **2012**, *134*, 10071; b) Z. He, C. Zhong, X. Huang, W.-Y. Wong, H. Wu, L. Chen, S. Su, Y. Cao, *Adv. Mater.* **2011**, *23*, 4636; c) PCE = 12.0% by Heliatek, www.heliatek.com; d) PCE = 11.0% by Mitsubishi Chemical, www.m-kagaku.co.jp; e) PCE = 10.6% by UCLA and Sumitomo Chemical; f) J. You, L. Dou, K. Yoshimura, T. Kato, K. Ohya, T. Moriarty, K. Emery, C.-C. Chen, J. Gao, G. Li, Y. Yang, *Nat. Commun.* **2013**, *4*, 1446.

[3] a) J. Min, Z.-G. Zhang, S. Zhang, Y. Li, *Chem. Mater.* **2012**, *24*, 3247; b) A. Najari, S. Beaupré, P. Berrouard, Y. Zou, J.-L. Pouliot, C. Lepage-Pérusse, M. Leclerc, *Adv. Funct. Mater.* **2011**, *21*, 718; c) Y. Liang, Z. Xu, J. Xia, S.-T. Tsai, Y. Wu, G. Li, C. Ray, L. Yu, *Adv. Mater.* **2010**, *22*, E135.

[4] a) G. C. Welch, R. C. Bakus II, S. J. Teat, G. C. Bazan, *J. Am. Chem. Soc.* **2013**, *135*, 2298; b) H. N. Tsao, D. M. Cho, I. Park, M. R. Hansen, A. Mavrinskiy, D. Y. Yoon, R. Graf, W. Pisula, H. W. Spiess, K. Müllen, *J. Am. Chem. Soc.* **2011**, *133*, 2605; c) J. K. Lee, W. L. Ma, C. J. Brabec, J. Yuen, J. S. Moon, J. Y. Kim, K. Lee, G. C. Bazan, A. J. Heeger, *J. Am. Chem. Soc.* **2008**, *130*, 3619.

[5] a) Y. Sun, J. H. Seo, C. L. Takacs, J. Seifter, A. J. Heeger, *Adv. Mater.* **2011**, *23*, 1679; b) K. X. Steirer, P. F. Ndione, N. E. Widjonarko, M. T. Lloyd, J. Meyer, E. L. Ratcliff, A. Kahn, N. R. Armstrong, C. J. Curtis, D. S. Ginley, J. J. Berry, D. C. Olson, *Adv. Energy Mater.* **2011**, *1*, 813; c) S. H. Park, A. Roy, S. Beaupré, S. Cho, N. Coates, J. S. Moon, D. Moses, M. Leclerc, K. Lee, A. J. Heeger, *Nat. Photonics* **2009**, *3*, 297.

[6] a) Y. Fu, H. Cha, G.-Y. Lee, B. J. Moon, C. E. Park, T. Park, *Macromolecules* **2012**, *45*, 3004; b) J. Liu, H. Choi, J. Y. Kim, C. Bailey, M. Durstock, L. Dai, *Adv. Mater.* **2012**, *24*, 538; c) D. Mori, H. Benten, H. Ohkita, S. Ito, K. Miyake, *ACS Appl. Mater. Interfaces* **2012**, *4*, 3325.

[7] a) L. Biniek, B. C. Schroeder, J. E. Donaghey, N. Yaacobi-Gross, R. S. Ashraf, Y. W. Soon, C. B. Nielsen, J. R. Durrant, T. D. Anthopoulos, I. McCulloch, *Macromolecules* **2013**, *46*, 727; b) I. Osaka, T. Abe, M. Shimawaki, T. Koganezawa, K. Takimiya, *ACS Macro Lett.* **2012**, *1*, 437; c) E. Jin, C. Du, M. Wang, W. Li, C. Li, H. Wei, Z. Bo, *Macromolecules* **2012**, *45*, 7843; d) J. D. Yuen, J. Fan, J. Seifter, B. Lim, R. Hufschmid, A. J. Heeger, F. Wudl, *J. Am. Chem. Soc.* **2011**, *133*, 20799.

[8] a) B. Burkhart, P. P. Khlyabich, B. C. Thompson, *ACS Macro Lett.* **2012**, *1*, 660; b) X. Guo, R. P. Ortiz, Y. Zheng, M.-G. Kim, S. Zhang, Y. Hu, G. Lu, A. Facchetti, T. J. Marks, *J. Am. Chem. Soc.* **2011**, *133*, 13685; c) X. Guo, H. Xin, F. S. Kim, A. D. T. Liyanage, S. A. Jenekhe, M. D. Watson, *Macromolecules* **2011**, *44*, 269; d) Y. Zou, A. Najari, P. Berrouard, S. Beaupré, B. R. Aích, Y. Tao, M. Leclerc, *J. Am. Chem. Soc.* **2010**, *132*, 5330; e) C. Piliego, T. W. Holcombe, J. D. Douglas, C. H. Woo, P. M. Beaujuge, J. M. J. Fréchet, *J. Am. Chem. Soc.* **2010**, *132*, 7595.

[9] a) Z. Ma, E. Wang, M. E. Jarvid, P. Henriksson, O. Inganäs, F. Zhang, M. R. Andersson, *J. Mater. Chem.* **2012**, *22*, 2306; b) R. Stalder, C. Grand, J. Subbiah, F. So, R. Reynolds, *Polym. Chem.* **2012**, *3*, 89; c) J. Mei, D. H. Kim, A. L. Ayzner, M. F. Toney, Z. Bao, *J. Am. Chem. Soc.* **2011**, *133*, 20130.

[10] a) W. Li, W. S. C. Roelofs, M. M. Wienk, R. A. J. Janssen, *J. Am. Chem. Soc.* **2012**, *134*, 13787; b) A. T. Yiu, P. M. Beaujuge, O. P. Lee, C. H. Woo, F. Michael, M. F. Toney, J. M. J. Fréchet, *J. Am. Chem. Soc.* **2012**, *134*, 2180; c) H. Bronstein, Z. Chen, R. S. Ashraf, W. Zhang, J. Du, J. R. Durrant, P. S. Tuladhar, K. Song, S. E. Watkins, Y. Geerts, M. M. Wienk, R. A. J. Janssen, T. Anthopoulos, H. Sirringhaus, M. Heeney, I. McCulloch, *J. Am. Chem. Soc.* **2011**, *133*, 3272.

[11] a) Y. Lin, H. Fan, Y. Li, X. Zhan, *Adv. Mater.* **2012**, *24*, 3087; b) X. Guo, M. Zhang, L. Huo, C. Cui, Y. Wu, J. Hou, Y. Li, *Macromolecules* **2012**, *45*, 6930; c) M. Zhang, X. Guo, Y. Li, *Macromolecules* **2011**, *44*, 8798.

[12] a) Y. Li, *Acc. Chem. Res.* **2012**, *45*, 723; b) S. V. Mierloo, A. Hadipour, M.-J. Spijkman, N. Van den Brande, B. Ruttens, J. Kesters, J. D'Haen, G. Van Assche, D. M. de Leeuw, T. Aernouts, J. Manca, L. Lutsen, D. J. Vanderzande, M. Maes, *Chem. Mater.* **2012**, *24*, 587; c) I. Osaka, M. Saito, H. Mori, T. Koganezawa, K. Takimiya, *Adv. Mater.* **2012**, *24*, 425; d) S. Subramaniyan, H. Xin, F. S. Kim, S. Shoaee, J. R. Durrant, S. A. Jenekhe, *Adv. Energy Mater.* **2011**, *1*, 854.

[13] a) I. Osaka, K. Takimiya, R. D. McCullough, *Adv. Mater.* **2010**, *22*, 4993; b) A. Bhuwalka, J. F. Mike, M. He, J. J. Intemann, T. Nelson, M. D. Ewan, R. A. Roggers, Z. Lin, M. Jeffries-EL, *Macromolecules* **2011**, *44*, 9611; c) E. Ahmed, R. S. Kim, H. Xin, S. A. Jenekhe, *Macromolecules* **2009**, *42*, 8615; d) M. M. Alam, S. A. Jenekhe, *Chem. Mater.* **2004**, *16*, 4647.

[14] E. Ahmed, S. Subramaniyan, F. S. Kim, H. Xin, S. A. Jenekhe, *Macromolecules* **2011**, *44*, 7207.

[15] G. Ren, C. W. Schlenker, E. Ahmed, S. Subramaniyan, S. Olthof, A. Kahn, D. S. Ginger, S. A. Jenekhe, *Adv. Funct. Mater.* **2013**, *23*, 1238.

[16] S. Subramaniyan, F. S. Kim, G. Ren, H. Li, S. A. Jenekhe, *Macromolecules* **2012**, *45*, 9029.

[17] a) R. Stalder, J. Mei, J. Subbiah, C. Grand, L. A. Estrada, F. So, J. R. Reynolds, *Macromolecules* **2011**, *44*, 6303; b) B. C. Popere, A. M. D. Pelle, S. Thayumanavan, *Macromolecules* **2011**, *44*, 4767; c) H. Yan, Z. Chen, Y. Zheng, C. Newman, J. R. Quinn, F. Dötz, M. Kastler, A. Facchetti, *Nature* **2009**, *457*, 679.

[18] a) J.-L. Brédas, D. Beljonne, V. Coropceanu, J. Cornil, *Chem. Rev.* **2004**, *104*, 4971; b) M. C. Scharber, D. Mühlbacher, M. Koppe, P. Denk, C. Waldauf, A. J. Heeger, C. J. Brabec, *Adv. Mater.* **2006**, *18*, 789.

[19] J. D. Yuen, J. Fan, J. Seifter, B. Lim, R. Hufschmid, A. J. Heeger, F. Wudl, *J. Am. Chem. Soc.* **2011**, *133*, 20799.

[20] a) A. Saeki, Y. Koizumi, T. Aida, S. Seki, *Acc. Chem. Res.* **2012**, *45*, 1193; b) F. C. Grozema, L. D. A. Siebbeles, *J. Phys. Chem. Lett.* **2011**, *2*, 2951; c) W. L. Rance, A. J. Ferguson, T. McCarthy-Ward, M. Heeney, D. S. Ginley, D. C. Olson, G. Rumbles, N. Kopidakis, *ACS Nano* **2011**, *5*, 5635; d) A. Saeki, Y. Yamamoto, Y. Koizumi, T. Fukushima, T. Aida, S. Seki, *J. Phys. Chem. Lett.* **2011**, *2*, 2549.

[21] A. Saeki, M. Tsuji, S. Seki, *Adv. Energy Mater.* **2011**, *1*, 661.

[22] A. Saeki, S. Yoshikawa, M. Tsuji, Y. Koizumi, M. Ide, C. Vijayakumar, S. Seki, *J. Am. Chem. Soc.* **2012**, *134*, 19035.

[23] Reviews: a) T. M. Clarke, J. R. Durrant, *Chem. Rev.* **2010**, *110*, 6736; b) X.-Y. Zhu, Q. Yang, M. Muntwiler, *Acc. Chem. Res.* **2009**, *42*, 1779.

[24] a) F. Etzold, I. A. Howard, R. Mauer, M. Meister, T.-D. Kim, K.-S. Lee, N. S. Baek, F. Laquai, *J. Am. Chem. Soc.* **2011**, *133*, 9469; b) K. Vandewal, A. Gadisa, W. D. Oosterbaan, S. Bertho, F. Banishoeib, I. Van Severen, L. Lutsen, T. J. Cleij, D. Vanderzande, J. V. Manca, *Adv. Funct. Mater.* **2008**, *18*, 2064.

[25] a) L. G. Kaake, J. J. Jasieniak, R. C. Bakus II, G. C. Welch, D. Moses, G. C. Bazan, A. J. Heeger, *J. Am. Chem. Soc.* **2012**, *134*, 19828; b) H. Ohkita, S. Cook, Y. Astuti, W. Duffy, S. Tierney, W. Zhang, M. Heeney, I. McCulloch, J. Nelson, D. D. C. Bradley, J. R. Durrant, *J. Am. Chem. Soc.* **2008**, *130*, 3030.

[26] a) B. Balan, C. Vijayakumar, A. Saeki, Y. Koizumi, S. Seki, *Macromolecules* **2012**, *45*, 2709; b) J. Kim, Y. S. Kwon, W. S. Shin, S.-J. Moon, T. Park, *Macromolecules* **2011**, *44*, 1909; c) Y. Li, Y. Chen, X. Liu, Z. Wang, X. Yang, Y. Tu, X. Zhu, *Macromolecules* **2011**, *44*, 6370;

d) W. Yue, Y. Zhao, H. Tian, D. Song, Z. Xie, D. Yan, Y. Geng, F. Wang, *Macromolecules* **2009**, *42*, 6510.

[27] a) T. Lei, Y. Cao, X. Zhou, Y. Peng, J. Bian, J. Pei, *Chem. Mater.* **2012**, *24*, 1762; b) I. Osaka, M. Shimawaki, H. Mori, I. Doi, E. Miyazaki, T. Koganezawa, K. Takimiya, *J. Am. Chem. Soc.* **2012**, *134*, 3498; c) I. Osaka, T. Abe, S. Shinamura, K. Takimiya, *J. Am. Chem. Soc.* **2011**, *133*, 6852.

[28] a) A. Saeki, T. Fukumatsu, S. Seki, *Macromolecules* **2011**, *44*, 3416; b) T. Fukumatsu, A. Saeki, S. Seki, *Appl. Phys. Express* **2012**, *5*, 061701.

[29] T. Yanai, D. P. Tew, N. C. Handy, *Chem. Phys. Lett.* **2004**, *393*, 51.

[30] a) Y.-J. Cheng, S.-H. Yang, C.-S. Hsu, *Chem. Rev.* **2009**, *109*, 5868; b) S. A. Jenekhe, L. Lu, M. M. Alam, *Macromolecules* **2001**, *34*, 7315; c) C. Kitamura, S. Tanaka, Y. Yamashita, *Chem. Mater.* **1996**, *8*, 570.

[31] P. A. Troshin, D. K. Susarova, Y. L. Moskvin, I. E. Kuznetsov, S. A. Ponomarenko, E. N. Myshkovskaya, K. A. Zakharcheva, A. A. Balakai, S. D. Babenko, V. F. Razumov, *Adv. Funct. Mater.* **2010**, *20*, 4351.

[32] a) Y.-J. Cheng, C.-H. Hsieh, P.-J. Li, C.-S. Hsu, *Adv. Funct. Mater.* **2011**, *21*, 1723; b) V. Chellappan, G. M. Ng, M. J. Tan, W.-P. Goh, F. Zhu, *Appl. Phys. Lett.* **2009**, *95*, 263305; c) Y. Kim, S. Cook, S. M. Tuladhar, S. A. Choulis, J. Nelson, J. R. Durrant, D. D. C. Bradley, M. Gile, I. McCulloch, C.-S. Ha, M. Ree, *Nat. Mater.* **2006**, *5*, 197.

[33] a) A. Garcia, G. C. Welch, E. L. Ratcliff, D. S. Ginley, G. C. Bazan, D. C. Olson, *Adv. Mater.* **2012**, *24*, 5368; b) W. Tress, K. Leo, M. Riede, *Adv. Funct. Mater.* **2011**, *21*, 2140.

[34] Y. Sun, C. J. Takacs, S. R. Cowan, J. H. Seo, X. Gong, A. Roy, A. J. Heeger, *Adv. Mater.* **2011**, *23*, 2226.

[35] a) Y. Maeyoshi, A. Saeki, S. Suwa, M. Omichi, H. Marui, A. Azano, S. Tsukuda, M. Sugimoto, A. Kishimura, K. Kataoka, S. Seki, *Sci. Rep.* **2012**, *2*, 600; b) J. Kim, G. Kim, Y. Choi, J. Lee, S. H. Park, K. Lee, *J. Appl. Phys.* **2012**, *111*, 114511; c) J. H. Kim, S. H. Kim, H.-H. Lee, K. Lee, W. Ma, X. Gong, A. J. Heeger, *Adv. Mater.* **2006**, *18*, 572.

[36] a) T. S. van der Poll, J. A. Love, T.-Q. Nguyen, G. C. Bazan, *Adv. Mater.* **2012**, *24*, 3646; b) K. R. Graham, P. M. Wieruszewski, R. Stalder, M. J. Hartel, J. Mei, R. So, J. R. Reynolds, *Adv. Funct. Mater.* **2012**, *22*, 4801; c) B. Verreet, B. P. Rand, D. Cheyns, A. Hadipour, T. Aernouts, P. Heremans, A. Medina, C. G. Claessens, T. Torres, *Adv. Energy Mater.* **2011**, *1*, 565.